Hindawi
Andrologia
Volume 2024, Article ID 6673310, 9 pages
https://doi.org/10.1155/2024/6673310

Research Article

A Biallelic Mutation in *CCDC103* Impairs Sperm Motility due to the Absence of Dynein Arms

Yi Yu,[1] **Jin-De Zhu**,[2] **Peng-Fei Liu**,[2] **Ming-Wei Zhan**,[2] **Bang-Xu Zheng**,[3] **Yu-Qi Lai**,[2] **Ke-Rong Wu**,[4] **and Xue-Jun Shang**[2]

[1]*Center of Reproductive Medicine, The First Affiliated Hospital of Ningbo University, Ningbo 315012, China*
[2]*Department of Urology, Jinling Hospital Affiliated to Nanjing University School of Medicine/General Hospital of Eastern Theater Command, Nanjing 210002, China*
[3]*Center of Reproductive Medicine, Ningbo Women and Children Hospital, Ningbo 31500, China*
[4]*Department of Urology, The First Affiliated Hospital of Ningbo University, Ningbo 315012, China*

Correspondence should be addressed to Ke-Rong Wu; wkr1983@163.com and Xue-Jun Shang; shangxj98@sina.com

Received 24 June 2023; Revised 19 March 2024; Accepted 8 April 2024; Published 26 April 2024

Academic Editor: Yong-Gang Duan

Primary ciliary dyskinesia (PCD) is a rare genetic condition characterized by destructive respiratory disease and laterality abnormalities due to randomized left–right body asymmetry. In men, PCD is also often associated with infertility due to immotile sperm owing to a malfunction of the sperm flagella. Pathogenic mutations have been found in more than 50 genes. Nonetheless, not all patients with PCD experience infertility. Therefore, to better understand the impact of PCD-associated mutations on male fertility, it is necessary to clarify the role of these genes in spermatogenesis. The *CCDC103* p.His154Pro mutation has a high prevalence in PCD. Here, we present the identification and functional analysis of a biallelic mutation in *CCDC103* identified in a familial case of PCD associated with male infertility. The biallelic *CCDC103* mutations, NM_213607:c.161_162del(p.His55Serfs*9) and NM_213607:c.461A > C (p.His154Pro), were identified by whole-exome sequencing. Sanger sequencing validation was performed on all available family members, and the mutation was recessively separated with an infertility phenotype. The c.161_162del mutation breaks the reading frame of the protein and, therefore, is predicted to produce a nonfunctional protein. The tertiary structure of *CCDC103*-mutated protein indicated a significant conformational change that likely affected protein function. Transmission electron microscopy of spermatozoa showed that both the mid and principal regions of the flagellum lacked dynein arms, which was confirmed via immunofluorescence staining. Using the method of laser-assisted immotile sperm selection combined with intracytoplasmic sperm injection, the patient's wife has a successful clinical pregnancy. These results extend the phenotype spectrum of the *CCDC103* mutation in PCD.

1. Introduction

Approximately 15%–20% of couples worldwide are experiencing problems with infertility. Primary ciliary dyskinesia (PCD, MIM244400), also known as cilia immobility syndrome, is an autosomal recessive inheritance disease [1]. The prevalence of PCD is from 1 : 10,000 to 1 : 20,000 live-born children [2]. In 1904, Siewart first reported a case of bronchiectasis with visceral inversion [3], a cilia dysfunction caused by various structural defects in the primary cilia. Primary ciliary motility disorders include immobility syndrome, Kartagener syndrome, ciliary dyskinesia, and primary ciliary orientation disorder [1]. The diseases caused by ciliary dysfunction are extensive and can affect all sites having distributed cilia. Respiratory tract infections caused by airway cilia dysfunction are the most common. In 1974, Afzelius found that patients with PCD had symptoms of impaired sperm motility in addition to bronchiectasis and the sinus tract [1].

The spermatozoa flagellar is composed of a "9 + 2" microtubule-based structure named the "axoneme" and is required for sperm motility [4]. The structure consists of two central microtubules and nine peripheral microtubule doublets.

The movement of cilia depends on dynein arms (DAs) composed of the outer (ODAs) and inner DAs (IDAs) in the outer axonal double-stranded microtubules [4]. The DA is a large protein complex consisting of several heavy, middle, and light chains. Structural abnormalities of microtubules, such as the absence of DA, resulting in axoneme disorder, can significantly reduce sperm motility [4, 5]. Although the motile cilia and sperm flagellar have similar axoneme structures, only half of PCD male patients have symptoms of low motility of sperm [3, 6], indicating the variability motility patterns of motile cilia and sperm flagella.

To date, approximately 50 known genes have been validated to be associated with PCD. In Chinese patients with PCD, dynein axonemal heavy chain 5 (DNAH5) is the most common pathogenic gene. In 2012, Panizzi et al. [7] first demonstrated that coiled-coil domain containing 103 (*CCDC103*) is a PCD pathogenic gene. As the *CCDC103* protein is tightly integrated within the axoneme and acts as a DA attachment [7, 8], it is vital for the motility of the cilia. Mutations in *CCDC103* cause PCD by disrupting the ciliary DA assembly.

Patients with PCD present various symptoms, including normal levels of nasal nitric oxide and partial and normal DA defects [8, 9]. The *CCDC103* p.His154Pro mutation has a high prevalence in South Asia [8]. In addition, it disrupts protein oligomerization [8, 9]. Previous study has shown that this mutation also affects sperm motility by disrupting the assembly of IDA and ODA [10]; however, the affected individuals described in these studies were diagnosed with asthenoteratozoospermia without any PCD symptoms. Thus, it remains unclear whether the *CCDC103* missense mutation affects fertility in patients with PCD.

In this study, a nonconsanguineous Chinese family was studied with an individual with PCD and asthenoteratozoospermia. Using whole exome sequencing (WES), we identified a compound heterozygous mutation in *CCDC103* (NM_213607: c.161_162del (p.His55Serfs*9), NM_213607: c.461A > C (p.His154Pro)) that was segregated recessively with an infertility phenotype. The results of transmission electron microscopy (TEM) and immunofluorescence staining showed a complete lack of DAs. Intracytoplasmic sperm injection (ICSI) was performed to select viable sperm for the patient. After two such interventions, the fertilization rate was 80.95% (17 sperm resulted in fertilization, 21 sperm were injected). Fortunately, the patient's spouse achieved a successful clinical pregnancy. These results extend the spectrum of the phenotype of the *CCDC103* mutation in PCD.

2. Participants and Methods

2.1. Participants and Clinical Data Evaluation. The patient had no clear family hereditary disorders according to a comprehensive medical history (Figure 1). Ultrasonography did not detect any positive signs of obstruction or inflammation in the testis or accessory sex glands. Routine semen analysis was performed via computer-assisted semen analysis three times following the 5th edition of the WHO Manual for the Laboratory Examination and Processing of Human Semen. Furthermore, eosin-nigrosin staining was used to assess sperm vitality. Before any procedure, we obtained written informed consent from the patient. The study was approved by the Institutional Ethical Committee of the Ningbo First Hospital with the approval number 2023-037A-02.

2.2. WES and Bioinformatic Analysis. Peripheral blood samples were used to extract total genomic DNA using DNeasy Blood and Tissue kits (Qiagen, Valencia, CA, USA). WES was prepared using the IDT xGen Exome Research Panel V1.0 (Integrated DNA Technologies, USA). The quantity and quality of sequencing libraries were evaluated using a Qubit 2.0 fluorometer (Thermo Fisher Scientific, Waltham, MA, USA) and a 2100 Bioanalyzer High Sensitivity DNA Assay (Agilent Technologies, Carlsbad, CA, USA). The qualified libraries were subjected to 2×150 bp paired-end sequencing on an Illumina NovaSeq platform (Illumina Inc., San Diego, CA, USA). FASTQ data were filtered and aligned to the human reference genome (hg19/GRCh37) using BWA v0.7.13. Mutations (including single nucleotide mutations and short insertions and deletions) were genotyped from recalibrated BAM files using GATK4.0 and annotated with ANNOVAR in multiple databases, including mutation descriptions, population frequencies, and mutation function predictions. The mutations were classified as pathogenic, likely pathogenic, mutations of unknown significance (VUS), likely benign, or benign, according to the American College of Medical Genetics guidelines. In addition, Sanger sequencing was performed for all family members using the primers listed in Table S1 specific for *CCDC103*.

2.3. 3D Reconstruction of the Mutant Protein. The FASTA sequence of the protein was downloaded from the UniProt database, and the amino acid sequence was uploaded to ITASSER for de novo modeling. Pymol2.3.0 was used for the reconstruction of the mutant protein and alignment. The mutant protein structure was superimposed on the wild-type protein structure.

2.4. Morphological Analysis of Sperm. Routine semen analysis was replicated three times. The semen collected from the patient was spread on slides and then fixed with 4% (*w*/*v*) paraformaldehyde (4% PFA; Servicebio Technology Co. Ltd., Wuhan, China) for 20 min, washed with phosphate-buffered saline (PBS) for 5 min, and stained with modified Papanicolaou solution (Xindi, Nanjing) for later morphological analysis. The percentages of morphologically normal and abnormal spermatozoa were evaluated according to the 5th edition of the WHO Manual for the Laboratory Examination and Processing of Human Semen. Representative images were captured by optical microscopy (Olympus, Japan).

2.5. Scanning Electron Microscopy (SEM) and TEM Analyses. A similar protocol was used in previous studies [4, 10]. Briefly, spermatozoa were washed with PBS and then fixed with 2.5% glutaraldehyde overnight. For SEM, spermatozoa blocks were washed with 0.1 M PBS (pH 7.4) three times for 15 min each. The blocks were then transferred to 1% OsO4 in 0.1 M PBS (pH 7.4) for 1–2 hr at room temperature and then washed in 0.1 M PBS (pH 7.4) three times for 15 min each. The samples were then dehydrated in 30%, 50%, 75%, 95%, and 100% ethanol for 15 min and filtered with isoamyl

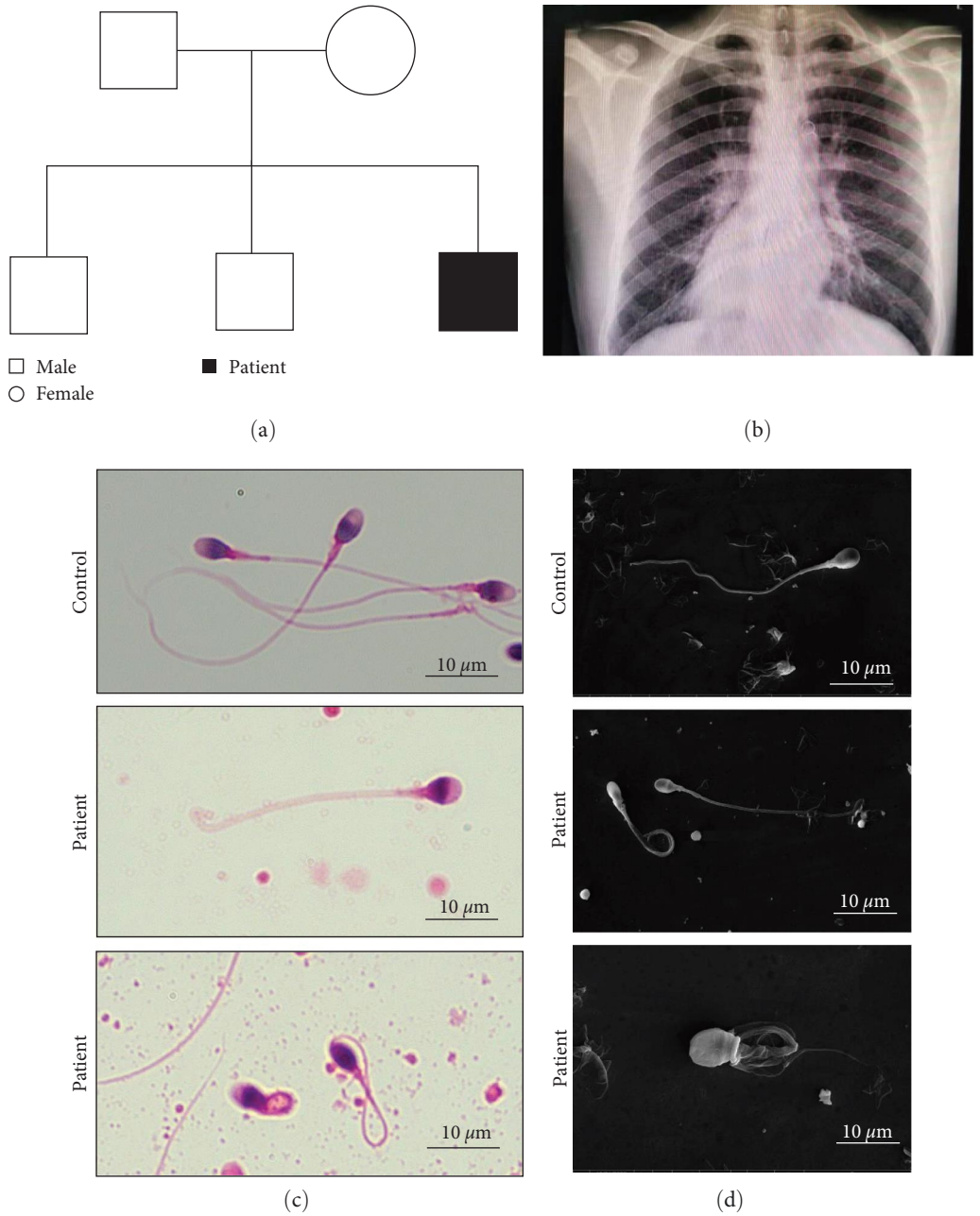

Figure 1: Clinical characteristics and sperm morphology of the patient. (a) Patient with male infertility from a Western Chinese family. (b) Radiographic inspection image shows the cardiac inversion of the patient. (c) Representative spermatozoa images from the fertile control and the patient. The spermatozoa of the patient showed a short, coiled, and bent tail. (d) Representative spermatozoa images of scanning electron microscopy (SEM) of a fertile control and the patient.

acetate. Afterward, the specimens were mounted on aluminum stubs, gold-coated by an ionic sprayer meter (Hitachi, Japan). Then, they were analyzed using a Nova Nano 450 Scanning Electron Microscope (Thermo FEI, USA) under an accelerating voltage of 10 kV.

For TEM, the fixed spermatozoa were rinsed with 1 × PBS buffer twice for 15 min each. Next, they were fixed with 1% osmic acid for 1 hr, rinsed with 1 × PBS buffer twice for 15 min, dehydrated with gradient ethanol, replaced with 100% acetone, and embedded in Epon 812 resin. Sections were cut at 1 μm intervals for orientation of the sperm flagellum. Subsequently, they were stained with uranyl acetate and lead citrate for 30 min. Finally, the spermatozoa ultrastructure was observed using a TECNAI-10 TEM (Philips, The Netherlands) under an accelerating voltage of 80 kV.

2.6. Immunofluorescence Staining. Immunofluorescence staining was performed as described in previous studies [5, 7]. Spermatozoa were fixed with 4% PFA for 20 min and then washed three times with 1 × PBS buffer for 10 min each. Then, they were blocked with 3% bovine serum albumin at room temperature for 30 min. The slides were then incubated

Table 1: Clinical characteristics of the patient.

Personal information	Semen paraments	Flagellum defects
Age, 26 years Height/weight, 175 cm/60 kg Infertility time, 3 years	Volume (mL), 3.25 ± 0.45	Coiled (%), 8–10
	Total sperm count ($\times 10^6$/time), 181.56 ± 1	Bent (%), 15–20
	Sperm concentration ($\times 10^6$/mL), 57 ± 8.2	Absent (%), 1–2.5
	Progressive motility (%), 0 ± 0	Short (%), 4.5 ± 1.5
	Sperm viability (%), 70 ± 2	Irregular caliber (%), 2 ± 0.5
	Normal sperm morphology (%), 2.35 ± 0.45	Multiple (%), 6 ± 1

Notes: Semen analysis was performed for three times. Semen paraments and flagellum defects data were presented as mean ± SEM, $n = 3$. Lower limit of the reference value. Volume (mL): 1.5 (1.4–1.7); Total sperm count ($\times 10^6$/time): 39 (34–46); Sperm concentration ($\times 10^6$/mL): 15 (12–16); Progressive motility (%): 32 (31–34); Sperm viability (%): 58 (55–63); Normal sperm morphology (%): 4 (3–4).

with primary antibody (Table S1) overnight at 4°C and placed in a wet box. The next day, the slides were washed with PBST three times and then incubated with secondary antibodies (Table S1) for 1 hr at room temperature. Finally, the slides were washed with PBST and stained with DAPI solution at room temperature for 10 min in the dark. All slides were observed under a confocal microscope (LEICA TCS-SP8, Germany), and images were captured. Negative controls were used to assess the specificity of all of the antibodies used.

2.7. Laser-Assisted Immotile Sperm Selection, ICSI, and Clinical Pregnancy Determination. The ovulation induction antagonist protocol was used to stimulate multiple follicular development for the patient's wife before the ICSI treatment. Following oocyte retrieval, the method of laser-assisted immotile sperm selection was employed to select immotile but viable spermatozoa, according to the previous report [11]. In brief, the procedure involves directing a single laser shot of 129 μJ for approximately 1.2 ms to the tip of the flagellum in live but immotile spermatozoa, resulting in the tail curling or coiling. Then, a single-viable spermatozoon was selected and being injected directly into the cytoplasm of the oocyte using a micropipette under high-magnification microscopy. The injected oocytes were then cultured in a controlled environment to allow for fertilization and early embryo development. Prior to the embryo transfer, the number and quality of embryos to be transferred were carefully assessed, taking into consideration factors such as embryo stage, morphology, and patient age. The transfer procedure was performed under ultrasound guidance to ensure accurate placement of the embryo(s) into the optimal location within the uterine cavity. To determine the clinical pregnancy after embryo transfer, a transvaginal ultrasound was performed 4 weeks after the transfer.

3. Results

3.1. Clinical Features and Sperm Morphology of the Patient. A Chinese patient with primary male infertility from a nonconsanguineous family was evaluated (Figure 1). The patient had a clear history of sinusitis and bronchiectasis combined with visceral inversion. Routine semen analysis suggested that the patient's spermatozoa were completely immobile, but his sperm vitality was greater than the reference value (Table 1). To discern the possible reason for the complete immobility, we evaluated the sperm morphology by modified Papanicolaou staining and SEM. Sperm abnormalities, including a coiled and bent flagellum, were observed. To explore the underlying mechanism, we performed a TEM analysis of the sperm, and the results showed that the middle and principal pieces of the flagellum lacked DA (Figure 2).

3.2. Biallelic Mutation in CCDC103. We employed WES to identify the genetic cause of the sperm flagellum defect. After filtering the FASTQ data according to the standard, a biallelic mutation was identified in *CCDC103* (NM_213607: c.161_162del, p.H55Sfs*9; c.461A > C, p.H154P) was identified (Table S2). Multiple sequence alignment in seven species indicated the conserved nature of amino acids 55 and 154 sites, and the seqlogo picture showed the amino acid frequency of each site near 55 and 154 sites in those seven species. We applied PyMol to reconstruct the tertiary structure of the *CCDC103* protein, and the results showed a significant change in the structure of the mutant protein (Figure 3(c)). For CCDC103p.His154Pro, as HIS was replaced by PRO, the hydrogen bond structure of length 1.9 between ALA-158 and HIS-154 disappeared, and the secondary structure of the *CCDC103* protein changed. Sanger sequencing validation was performed on all available family members and the mutation was recessively separated with an infertility phenotype (Figure S1). In addition, we have identified two potential pathogenic genes, NM_001372: c.5020G > A, p.G1674R; NM_001372: c.9560A > G, p.N3187S (Table S3). However, further family validation has ruled out the DNAH5 gene as the causative gene for the patient, as the patient's brother (who has normal fertility) and father (also with normal fertility) both carry these two mutations in the DNAH5 gene (Figure S2).

3.3. Absence of DAs Associated with CCDC103 Mutation. To confirm the absence of DAs in the patient, we performed an immunostaining analysis using DNAI2 antibodies (markers of outer DAs) and DNAH1 antibodies (markers of inner DAs) on spermatozoa from a fertile control and our patient (Figure 4). Significant signals of DNAI2 and DNAH1 were observed in the flagellum of the control spermatozoa. In contrast, no specific signals were observed in the patient's spermatozoa. These results, together with the TEM results (Figure 2), validated the dysfunctional DA assembly in the patient.

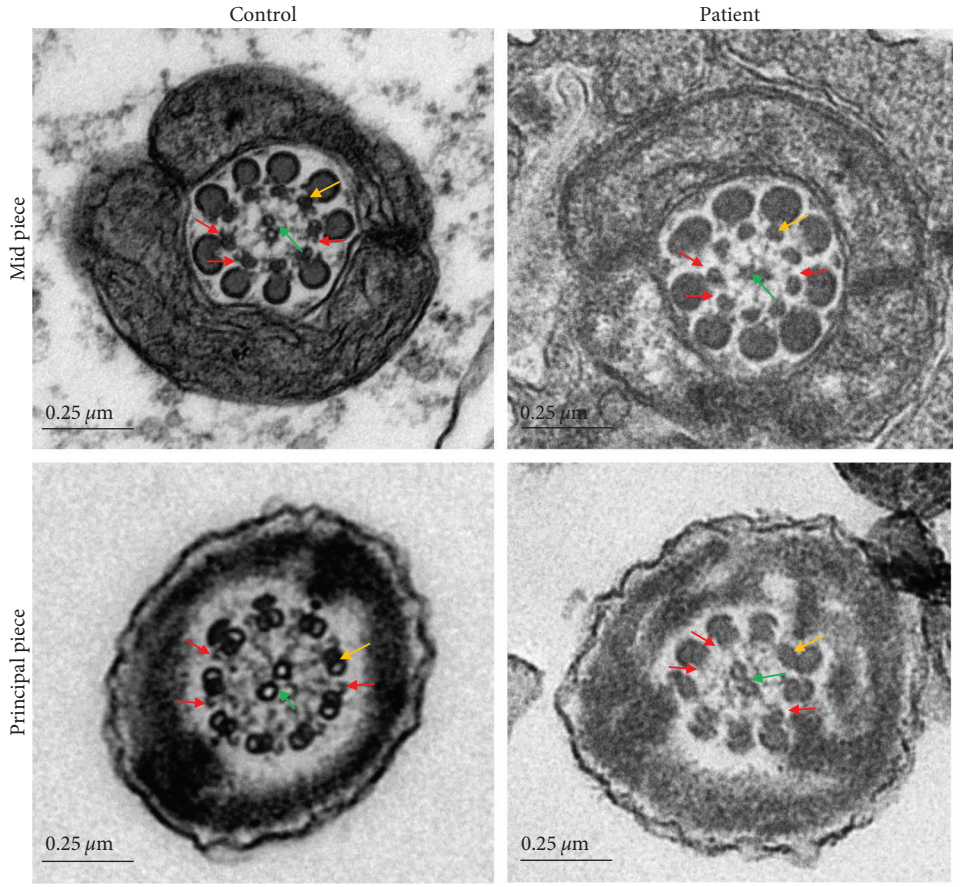

FIGURE 2: TEM analysis of spermatozoa from the patient with the *CCDC103* mutation shows the absence of dynein arms. Representative TEM image showing cross-sections of the middle and principal piece of sperm flagella from a fertile control and the patient. The green arrow indicates normal CP in the control and patient. The yellow arrow indicates normal DMTs in the control and patient. The red arrow indicates normal DAs in the control and the absence of DAs in the patient. TEM, transmission electron microscopy; *CCDC103*, coiled-coil domain-containing 103; DA, dynein arm. CP, central pair of microtubules; DMT, peripheral microtubule doublets. Scale bars = 0.2 μm.

3.4. Patients with CCDC103 Mutation Achieved a Successful Outcome of Assisted Reproductive Technology. The patient's wife underwent two cycles of ovulation induction treatment using an antagonist protocol, resulting in a total of 21 retrieved eggs. The embryologist used laser-assisted selection to select viable sperm and performed ICSI using the selected viable sperm. After two interventions, the fertilization rate was 80.95% (17 eggs resulted in fertilization out of 21 eggs injected with sperm). Finally, a total of three embryos were transplanted in two separate procedures, and the patient's wife gave birth to a healthy baby (Table 2).

4. Discussion

The rhythmic swinging of flagella is what powers the sperm. The flagella consists of three parts, including the middle, principal, and end regions. Each segment is generally composed of an axoneme, peripheral dense fibers, mitochondrial sheath, and cell membrane. Normal sperm axoneme consists of two central microtubules and nine pairs of peripheral double microtubules; this is known as the "9 + 2" structure. DAs, which contain the ATP enzyme, produce energy for the sliding of microtubules and to drive the movement of flagella. Defects of any axoneme structure may contribute to sperm immobility.

Currently, both intraflagellar transport (IFT) and intramanchette transport are believed to participate in flagella formation, although the former is considered the main mechanism [5, 12]. IFT is the key protein transport pathway of the cilia, through which many important proteins are transported [13]. Proteins in cytoplasmic synthesis are delivered to the axoneme site to participate in the synthesis of DAs and flagellar assembly [13]. Previous studies have reported that the absence of flagella transport-related proteins may lead to disruption of flagella formation and, therefore, impair sperm motility [14].

PCD is a genetic disease mainly characterized by respiratory symptoms such as chronic otitis media, sinusitis, bronchiectasis, and visceral inversion [1]. Some male patients with PCD also experience infertility due to the disruption of sperm flagella assembly [3, 15]. Ultrastructural changes in the respiratory tract cilia in patients with PCD are mainly DA defects, while few patients have defects in the cilia of the respiratory tract [16]. More than 50 pathogenic genes have

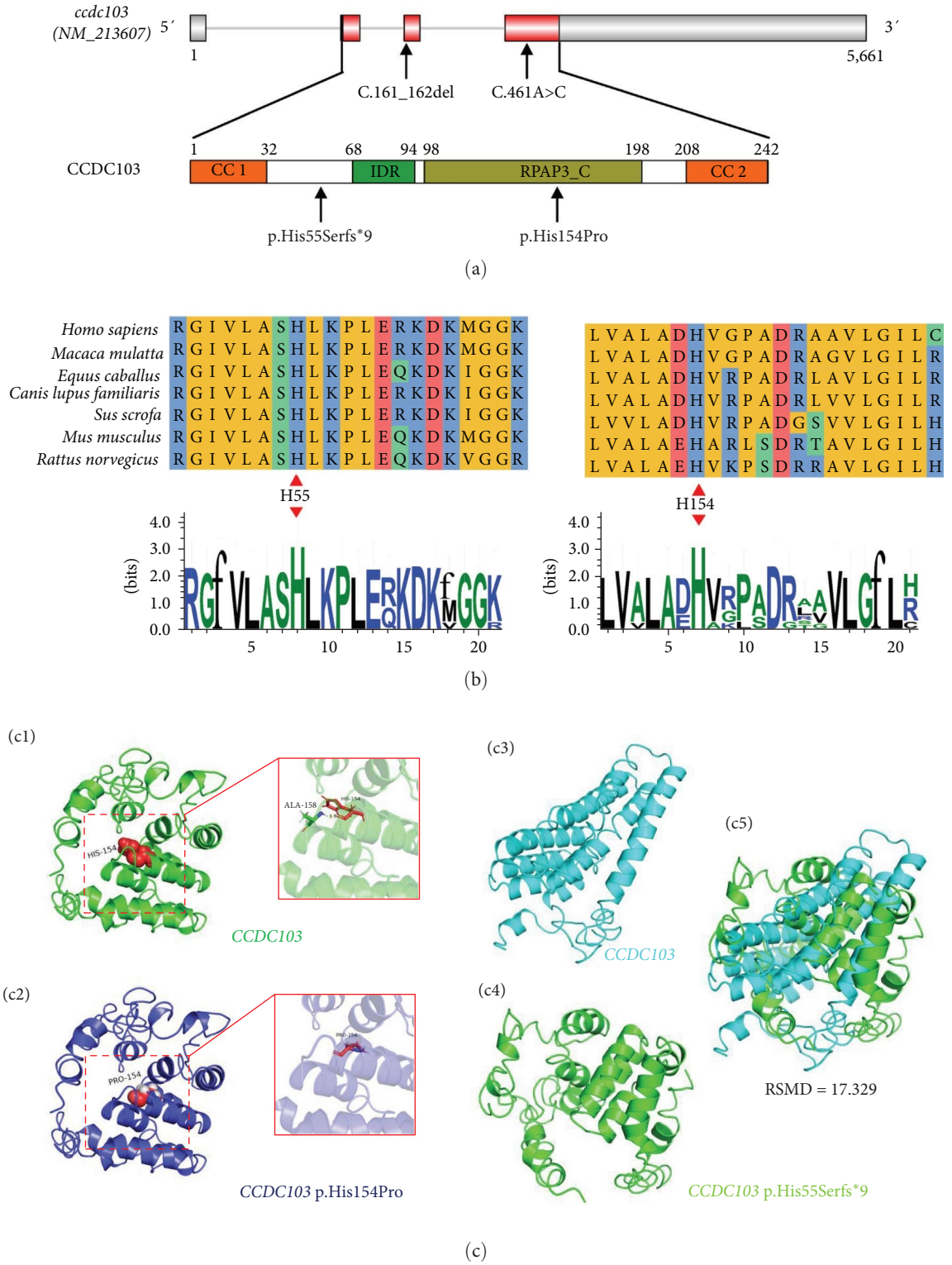

Figure 3: Amino acid conservation analysis of *CCDC103* and the 3D reconstruction of the CCDC103 protein. (a) Gene structure (top) and protein conserved domain analysis (bottom) in *CCDC103*. The red and gray rectangles represent exons and UTR structures, respectively, while the gray lines represent introns. Different protein-conserved domains are represented by rectangles of different colors. CC, coiled coils, IDR, coiled coils, RPAP3_C, N-terminal of the RPAP3_C domain. (b) Multiple sequence alignment of seven species indicating the conserved nature of amino acids 55 and 154 sites (above), and the seqlogo picture showed the amino acid frequency of each site near the 55 and 154 sites in these seven species (below). (c) c1: CCDC103 protein model: ALA-158 forms hydrogen bonds with HIS-154 with a length of 1.9. c2: CCDC103 p.His154Pro protein model. c3, c4: CCDC103 and CCDC103 p.His55Serfs*9 protein models, respectively. c5: Image c3 is superimposed onto the image of c4. The RMSD (root mean square deviation) is 17.329, indicating that the base deletion (c.161_162del) has a great influence on the protein structure.

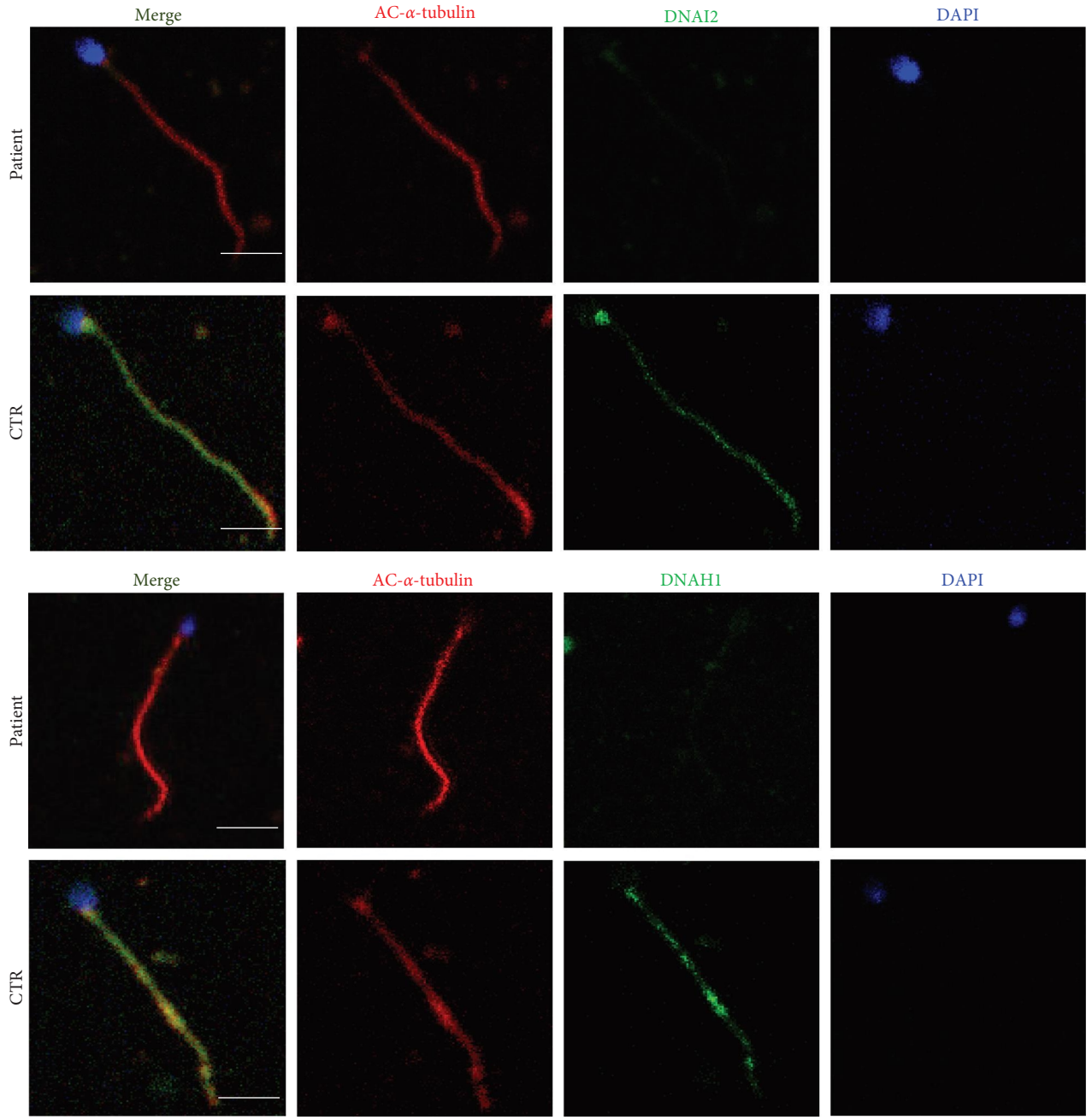

Figure 4: Immunofluorescence staining of the patient's sperm showed little expression of DNAI 2 or DNAH1 compared to the normal control sperm. Scale bars = 5 μm; CTR, control.

Table 2: Analysis of the outcome of assisted reproductive technology in patients with CCDC103 mutation.

Fertilization rate Fertilized/injected (D1)	High-quality embryos rate High-quality embryos/fertilized embryos (D3)	Blastocyst formation rate (D5) Blastocyst/high-quality embryos/(D5)	Clinical pregnancy Clinical pregnancy/transferred embryos
17/21	14/17	8/14	1/3

Notes: D1: 1 day after the intracytoplasmic sperm injection (ICSI); D3: 3 days after the intracytoplasmic sperm injection ICSI; D5: 5 days after the ICSI.

been associated with PCD, and the proteins they encode mainly affect the cilia assembly of DAs, axonemes, and the cytoskeleton [17, 18]. One study in France found that 37 of 49 men with PCD were also infertile, and the flagella of infertile men exhibited inner DA defects and structural microtubule disorders [17].

Among the pathogenic PCD genes, CCDC39 and CCDC40 are the most frequently reported in cases of PCD with infertility [6, 17]. In the French study [17], most infertility cases were caused by the CCDC40 gene mutation, which reached an incidence of about 43.2% (16/37) and mainly affected the assembly of the inner DA and microtubule structure, resulting in decreased sperm motility. However, in China, DNAH5 mutations are the most common, according to the latest review [19].

CCDC103 was first identified as a pathogenic PCD gene in 2012 [7]. In that study, the respiratory cilia of an affected individual with homozygous *CCDC103* loss-of-function mutations displayed variable defects in the outer DAs. The authors also observed that, in zebrafish embryos, *CCDC103* was expressed in both the cytoplasm and olfactory placode cilia. Furthermore, the fractionation of Chlamydomonas flagella showed that *Ccdc103*/*Pr46b* was expressed in the flagella and remained closely associated with the axonemes, indicating that *CCDC103* is tightly integrated within the axoneme and acts in DA attachment. However, it remains unknown whether individuals with PCD and with loss-of-function *CCDC103* mutations display infertility. Previous study has demonstrated that the *CCDC103* p.His154Pro mutation reduced sperm motility by interfering with the assembly of IDA and ODA in nonsyndromic asthenozoospermia [10]. However, the question of whether the *CCDC103* mutation leads to asthenozoospermia in patients with PCD remained unclear. In the present study, we report a case of a male patient with PCD with asthenozoospermia who inherited the *CCDC103* gene mutation from his parents (Figure S1 and Table S2). Furthermore, a high prevalence of the *CCDC103* p.His154Pro mutation has been reported in South Asian patients with PCD [9]. In our study, *CCDC103* p.His55Serfs*9 was first identified in individuals with PCD. The affected individual presented sinusitis, visceral inversion, and absolute asthenozoospermia. Ultrastructural changes in sperm in our patient were similar to those reported by Zubair et al. [10]. The spermatozoa of the patient lacked DAs in the mid and principal regions of the flagella, leading to a significant decrease in sperm motility.

Currently, ICSI is the predominant method for patients with PCD with infertility to have offspring, and the pregnancy success rate is 40.5% [17]. As the sperm of affected individuals have poor motility, evaluating sperm viability is crucial for sperm selection prior to ICSI. Sperm viability can be analyzed via different methods, such as the hypoosmotic swelling test, sperm tail flexibility test, and laser-assisted immotile sperm selection (LAISS) [20]. Both sperm viability and the type of ultrastructural defect may affect the success rate of ICSI. In general, affected individuals with low sperm viability and central pair defects of spermatozoa tend to have lower clinical pregnancy rates [2]. When sperm viability is poor, it is more appropriate to use testicular spermatozoa for ICSI. In our study, the patient had a sperm viability of 63%–68%, and the TEM analysis indicated the absence of DAs without any central pair or outer pair defects. Hence, we used the method of LAISS to select viable sperm for ICSI. The fertilization rate was 80.95% (17/21) and the patient's spouse achieved a successful clinical pregnancy.

While providing valuable insights into the phenotypic spectrum of CCDC103 mutations, these results may not be generalizable to all cases of PCD or male infertility. Establishing a direct causal relationship between this specific mutation and the observed phenotypes requires further experimental validation. In vitro functional assays and animal models could be employed to conclusively demonstrate the mechanistic impact of these mutations on sperm motility and ciliary function. Future studies with a larger and more diverse sample size are necessary to validate these findings across different populations.

5. Conclusions

In this study, we identified a compound heterozygous mutation in *CCDC103* (NM_213607: c.161_162del (p.His55Serfs*9), NM_213607: c.461A > C (p.His154Pro)) that was segregated recessively with an infertility phenotype in a Chinese PCD family, and thus this case expands the currently known mutation spectrum of the CCDC gene in patients with PCD. The TEM of the patient's spermatozoa indicated the absence of DAs in the mid and principal regions of the flagella. Using the LAISS method to select viable sperm for ICSI, the spouse of the patient has achieved a successful clinical pregnancy. Further prospective studies evaluating the genotype, sperm ultrastructural phenotype, and ART outcomes of males with PCD are required to improve fertility.

Data Availability

The data presented in this paper are available upon request from the corresponding author. The data are not publicly available due to privacy reasons.

Ethical Approval

The study was approved by the Institutional Ethical Committee of the Ningbo First Hospital with the approval number 2023-037A-02.

Consent

Informed consent was obtained from all subjects involved in the study. Written informed consent was obtained from the patient to publish this paper.

Conflicts of Interest

The authors declare that they have no conflicts of interest.

Authors' Contributions

Conceptualization was done by Yi Yu, Ke-Rong Wu and Xue-Jun Shang; Data curation was done by Bang-Xu Zheng and Yu-Qi Lai; Funding acquisition was done by Ke-Rong Wu, Bang-Xu Zheng, and Xue-Jun Shang; Investigation was

done by Jin-De Zhu and Peng-Fei Liu; Methodology was done by Yi Yu and Peng-Fei Liu; Project administration was done by Xue-Jun Shang; Resources were provided by Jin-De Zhu and Peng-Fei Liu; Software-related task was done by Yi Yu, Jin-De Zhu, Peng-Fei Liu, and Ming-Wei Zhan; Supervision was done by Xue-Jun Shang and Ke-Rong Wu; Visualization was done by Xue-Jun Shang; Writing–original draft was done by Yi Yu; Writing–review and editing was done by Yi Yu, Jin-De Zhu, and Xue-Jun Shang. Yi Yu, Jin-De Zhu, and Peng-Fei Liu contributed equally to this work.

Acknowledgments

The authors appreciate the Center of Cryo-Electron Microscopy, Zhejiang University, for performing TEM and SEM. This research was funded by Ningbo Clinical Research Center for Urological Disease (2019A21001); Ningbo Top Medical and Health Research Program (2022020203); Medical and Health Science and Technology Project of Zhejiang Province, grant number (2023KY1115).

Supplementary Materials

Table S1–S3 and Figure S1 and S2 were listed in the Supplementary Materials. (*Supplementary Materials*)

References

[1] M. R. Knowles, L. A. Daniels, S. D. Davis, M. A. Zariwala, and M. W. Leigh, "Primary ciliary dyskinesia. Recent advances in diagnostics, genetics, and characterization of clinical disease," *American Journal of Respiratory and Critical Care Medicine*, vol. 188, no. 8, pp. 913–922, 2013.

[2] V. Mirra, C. Werner, and F. Santamaria, "Primary ciliary dyskinesia: an update on clinical aspects, genetics, diagnosis, and future treatment strategies," *Frontiers in Pediatrics*, vol. 5, Article ID 135, 2017.

[3] C. N. Jayasena and A. Sironen, "Diagnostics and management of male infertility in primary ciliary dyskinesia," *Diagnostics*, vol. 11, no. 9, Article ID 1550, 2021.

[4] W. Li, H. Wu, F. Li et al., "Biallelic mutations in *CFAP65* cause male infertility with multiple morphological abnormalities of the sperm flagella in humans and mice," *Journal of Medical Genetics*, vol. 57, no. 2, pp. 89–95, 2020.

[5] Y. Yu, J. Wang, L. Zhou, H. Li, B. Zheng, and S. Yang, "CFAP43-mediated intra-manchette transport is required for sperm head shaping and flagella formation," *Zygote*, vol. 29, no. 1, pp. 75–81, 2021.

[6] Z.-Y. Ji, Y.-W. Sha, L. Ding, and P. Li, "Genetic factors contributing to human primary ciliary dyskinesia and male infertility," *Asian Journal of Andrology*, vol. 19, no. 5, pp. 515–520, 2017.

[7] J. R. Panizzi, A. Becker-Heck, V. H. Castleman et al., "*CCDC103* mutations cause primary ciliary dyskinesia by disrupting assembly of ciliary dynein arms," *Nature Genetics*, vol. 44, no. 6, pp. 714–719, 2012.

[8] S. M. King and R. S. Patel-King, "The oligomeric outer dynein arm assembly factor *CCDC103* is tightly integrated within the ciliary axoneme and exhibits periodic binding to microtubules," *Journal of Biological Chemistry*, vol. 290, no. 12, pp. 7388–7401, 2015.

[9] A. Shoemark, E. Moya, R. A. Hirst et al., "High prevalence of *CCDC103* p.His154Pro mutation causing primary ciliary dyskinesia disrupts protein oligomerisation and is associated with normal diagnostic investigations," *Thorax*, vol. 73, no. 2, pp. 157–166, 2018.

[10] M. Zubair, R. Khan, A. Ma et al., "A recurrent homozygous missense mutation in *CCDC103* causes asthenoteratozoospermia due to disorganized dynein arms," *Asian Journal of Andrology*, vol. 24, no. 3, pp. 255–259, 2022.

[11] V. Nordhoff, "How to select immotile but viable spermatozoa on the day of intracytoplasmic sperm injection? An embryologist's view," *Andrology*, vol. 3, no. 2, pp. 156–162, 2015.

[12] J. T. San Agustin, G. J. Pazour, G. B. Witman, and W. Marshall, "Intraflagellar transport is essential for mammalian spermiogenesis but is absent in mature sperm," *Molecular Biology of the Cell*, vol. 26, no. 24, pp. 4358–4372, 2015.

[13] K. F. Lechtreck, "IFT–cargo interactions and protein transport in cilia," *Trends in Biochemical Sciences*, vol. 40, no. 12, pp. 765–778, 2015.

[14] Y. Zhang, H. Liu, W. Li et al., "Intraflagellar transporter protein 140 (IFT140), a component of IFT-A complex, is essential for male fertility and spermiogenesis in mice," *Cytoskeleton (Hoboken)*, vol. 75, no. 2, pp. 70–84, 2018.

[15] A. Sironen, A. Shoemark, M. Patel, M. R. Loebinger, and H. M. Mitchison, "Sperm defects in primary ciliary dyskinesia and related causes of male infertility," *Cellular and Molecular Life Sciences*, vol. 77, no. 11, pp. 2029–2048, 2020.

[16] M. Kurkowiak, E. Ziętkiewicz, and M. Witt, "Recent advances in primary ciliary dyskinesia genetics," *Journal of Medical Genetics*, vol. 52, no. 1, pp. 1–9, 2015.

[17] G. J. Vanaken, L. Bassinet, M. Boon et al., "Infertility in an adult cohort with primary ciliary dyskinesia: phenotype–gene association," *European Respiratory Journal*, vol. 50, no. 5, Article ID 1700314, 2017.

[18] M. Goutaki and A. Shoemark, "Diagnosis of primary ciliary dyskinesia," *Clinics in Chest Medicine*, vol. 43, no. 1, pp. 127–140, 2022.

[19] B. Peng, Y.-H. Gao, J.-Q. Xie et al., "Clinical and genetic spectrum of primary ciliary dyskinesia in Chinese patients: a systematic review," *Orphanet Journal of Rare Diseases*, vol. 17, no. 1, Article ID 283, 2022.

[20] C. Ortega, G. Verheyen, D. Raick, M. Camus, P. Devroey, and H. Tournaye, "Absolute asthenozoospermia and ICSI: what are the options?" *Human Reproduction Update*, vol. 17, no. 5, pp. 684–692, 2011.